HTML ABSTRACT + LINKS

Composition and temperature dependence of cesium-borate glasses by molecular dynamics

Alice Vegiri, Cristos-Platon E. Varsamis,[a] and Efstratios I. Kamitsos
Theoretical and Physical Chemistry Institute, National Hellenic Research Foundation, 48 Vassileos Constantinou Avenue, Athens 11635, Greece

(Received 24 January 2005; accepted 6 May 2005; published online 14 July 2005)

The structural aspects of $x\mathrm{Cs_2O}$-$(1-x)\mathrm{B_2O_3}$ glasses have been investigated by molecular dynamics as functions of $\mathrm{Cs_2O}$ content ($x=0.2$, 0.3, and 0.4) and temperature ($T=300$ and 1250 K). The tetrahedral ($\mathrm{B}\emptyset_4^-$) and triangular ($\mathrm{B}\emptyset_3$, $\mathrm{B}\emptyset_2\mathrm{O}^-$, and $\mathrm{B}\emptyset\mathrm{O}_2^{2-}$) short-range order borate units were found to be the structure-building entities of the simulated glasses [Ø=bridging oxygen (BO) and O^-=nonbridging oxygen (NBO) atom]. The increase of $\mathrm{Cs_2O}$ content results in the progressive increase of the NBO-containing triangle population at the expense of the $\mathrm{B}\emptyset_4^-$ tetrahedral units. The same effect is caused by temperature increase at a fixed $\mathrm{Cs_2O}$ content, and this was associated with the "fragile" characteristics of alkali borate glasses. A comparison of simulated Cs and Li borates showed very similar structures at $x=0.2$, but dissimilar ones when the alkali content exceeds this composition. In particular, for $x>0.2$ Cs borates exhibit a preference for NBO formation relative to Li borates. Differences in the microstructure of sites hosting Cs ions were found, and this permits their classification into bridging (*b* type) and nonbridging type (nb type) of sites. *b*-type sites consist exclusively of BO atoms, while both BO and NBO atoms participate in nb-type sites. These differences in Cs-site local bonding characteristics were found to be reflected on the Cs–O(site) vibration frequencies. Also, the computed Cs–O vibrational responses for simulated Cs borates were found to compare well with experimental far-infrared spectra. © *2005 American Institute of Physics*. [DOI: 10.1063/1.1943414]

I. INTRODUCTION

Alkali and alkaline-earth borate glasses are characterized by nonmonotonic variations of physical properties with metal oxide content, a phenomenon known as the "boron anomaly" effect. Early studies on borate glasses aimed at elucidating the nature and relative population of the borate units comprising the glass network as a means of providing a structural basis for explaining the boron anomaly effect.[1] The works of Krogh-Moe by infrared,[2] Bray and co-workers by NMR,[3–5] and Konijnendijk and Stevels by Raman spectroscopy[6] have made pioneering contributions in this field. While glassy $\mathrm{B_2O_3}$ is known to result from interconnected $\mathrm{B}\emptyset_3$ triangles (Ø denotes an oxygen atom bridging two boron centers), a fraction of which is being arranged in planar boroxol rings,[2–8] addition of metal oxide to boron oxide was found to cause the transformation of neutral $\mathrm{B}\emptyset_3$ units into charged $\mathrm{B}\emptyset_4^-$ tetrahedra. For alkali borate glasses, $x\mathrm{M_2O}$-$(1-x)\mathrm{B_2O_3}$ (M=alkali), the early studies showed that for $x<0.30$ the fraction of $\mathrm{B}\emptyset_4^-$ units N_4, follows the law $N_4=x/(1-x)$; i.e., each added oxygen atom converts two $\mathrm{B}\emptyset_3$ units into two $\mathrm{B}\emptyset_4^-$ tetrahedra, but N_4 was found to be independent of the nature of alkali metal ion.[3–5] For alkali modifier contents above ca. $x=0.30$ the network modification involves mainly the formation of nonbridging oxygen atoms (NBO) on borate triangular units, with the number of NBOs increasing progressively as x changes towards $x=0.75$. These units are the metaborate triangles $\mathrm{B}\emptyset_2\mathrm{O}^-$, pyroborate dimers $\mathrm{B_2}\emptyset\mathrm{O}_4^{4-}$, and orthoborate monomers BO_3^{3-}.

In addition to the strong influence of the metal oxide content, studies of physical properties of borate glasses have shown a clear dependence on the type of alkali modifier as well. This is demonstrated by viscosity,[9] absorption edge,[10] optical basicity,[11,12] glass transition temperature, and thermal-expansion coefficient[13,14] data of alkali borate glasses. It is possible that this dependence on the type of $\mathrm{M_2O}$ oxide originates from structural variations, although less pronounced than those induced by the increasing $\mathrm{M_2O}$ modifier content. For example, the viscosity–composition isotherms have been discussed in terms of the field strength of the alkali metal ion, and it has been suggested that for a given $\mathrm{M_2O}$ content the concentration of NBOs increases from Li to Cs.[9] This trend is consistent with the alkali dependence of other physical properties,[10–14] including sound velocities and elastic constants which decrease systematically as the alkali changes from Li to Cs.[15]

Such a disagreement for the role of metal ions, resulted from parallel studies of the structure and properties of alkali borate glasses, appeared to be resolved in more recent NMR investigations of Zhong and Bray[16] and Bray.[17] By employing wide-line ^{11}B NMR with more sensitive instrumentation and signal-averaging techniques, they were able to demonstrate that N_4 follows the theoretical curve $x/1-x$ for alkali contents lower than ca. $x=0.15$, but for glasses with larger alkali contents N_4 is a strong function of the alkali ion. In

[a]Author to whom correspondence should be addressed. Fax: +30-210-7273-794. Electronic mail: cvars@eie.gr

 © 2005 American Institute of Physics

Downloaded 08 Dec 2008 to 194.177.215.121. Redistribution subject to AIP license or copyright; see http://jcp.aip.org/jcp/copyright.jsp

particular, they found the N_4 fraction to decrease as the size of the alkali metal ion increases.[16,17] This result reflects a competition between the two transformation processes in the composition range $x \geqslant 0.15$, i.e., the parallel formation of $B\emptyset_4^-$ tetrahedra and NBO-containing borate triangles. A similar dependence of the borate structure on alkali metal type was revealed by Raman[18] and infrared[19,20] spectroscopy, as well as by molecular-dynamics simulations of borate glasses.[21,22] Youngman and Zwanziger[23] concluded from their ^{11}B dynamic-angle spinning (DAS) NMR study of Rb borate glasses that the N_4 values were consistent with those determined in the NMR study of Zhong and Bray[16] and Bray.[17] Also, a recent neutron-scattering study by Majerus *et al.* showed that N_4 decreases progressively from Li to K for alkali borate glasses with composition $x=0.33$.[24]

The structure of cesium borate glasses was reinvestigated recently by Berryman *et al.* employing ^{11}B NMR spectroscopy.[25] It was found that the N_4 values for Cs borate glasses follow closely those determined for glasses in the Li borate system, while in the earlier Zhong and Bray study a clear difference was revealed in N_4 values between the two systems.[16,17] Kodama and Kojima[26] reported high-precision ultrasonic velocity data for Cs and Li borate glasses and modeled the elastic properties in terms of the population and elastic constants of three local structural units: $B\emptyset_3$, $B\emptyset_4^-M^+$, and $B\emptyset_2O^-M^+$. Their property–structure analysis showed that the N_4 parameter follows the relation $N_4=x/(1-x)$ for Li borates in the range $0 \leqslant x \leqslant 0.28$ and deviates from this relation at higher lithium contents. This suggests that the conversion of $B\emptyset_3$ to $B\emptyset_4^-$ units takes place for compositions up to ca. $x=0.28$, and this process is followed by the decay of $B\emptyset_4^-$ and the formation of $B\emptyset_2O^-$ units for $x>0.28$. The results obtained for Cs borate glasses were quite distinct in that the deviation of N_4 from the $x/(1-x)$ relation was observed at very low Cs_2O contents, i.e., at ca. $x=0.065$.[26] This finding was taken to demonstrate a larger tendency of Cs borate glasses for nonbridging oxygen formation in comparison to Li borates of the same alkali content. In view of these points, we note that a recent ^{11}B magic-angle spinning (MAS) NMR study by Clarida *et al.*[27] of borate glasses with alkali content $x=0.286$ has suggested that N_4 has little or no dependence on the type of alkali metal, though the measured values are systematically higher than 0.40, corresponding to the $x/(1-x)$ value. It is apparent that more work is required in this field to shed light on the structural peculiarities exhibited by modified borate glasses.

We have recently employed molecular-dynamics (MD) simulations to investigate structural aspects and ion dynamics in Li borate glasses.[28–30] The analysis of the MD data allowed the evaluation of the relative population of the local structural units as a function of lithium oxide content and temperature. In addition, the microstructure of sites hosting Li ions was studied, and the corresponding Li ion site vibrational response was computed and compared with experimental far-infrared spectra. In this work we extend our MD studies to cesium borate glasses xCs_2O-$(1-x)B_2O_3$ as a function of composition ($x=0.2$, 0.3, and 0.4) and temperature ($T=300$ and 1250 K). In the first part of the work we focus on the structure of the simulated glasses, expressed by the molar fractions of the short-range-order (SRO) structural units, and on the dependence of this structure on composition and temperature. The results are compared with those obtained for Li borate glasses under similar conditions in order to search for any influence of the alkali metal ion on the SRO structure of a glass. The structural information is subsequently employed to determine the types of site occupied by Cs ions and to calculate the short-time dynamics related to the rattling motion of Cs ions in their local sites. The results are discussed in comparison with previous reports on the structure and properties of glasses in the Cs borate system.

II. COMPUTATIONAL METHOD

The MD simulations were performed on a collection of ca. 512 atoms in a primitive cubic lattice, with lattice parameters calculated from the experimental density data of Cs borate glasses.[31–33] Interatomic interactions were treated by means of the usual Born–Mayer–Huggins potential,[21]

$$V_{ij}(r) = A_{ij} \exp(-r/\rho) + z_i z_j e^2/r, \tag{1}$$

where

$$A_{ij} = 20.3545\left(1 + \frac{z_i}{\eta_i} + \frac{z_j}{\eta_j}\right)\exp\left(\frac{r_i + r_j}{\rho}\right) \quad \text{(kJ/mol)}. \tag{2}$$

In Eqs. (1) and (2), $z_i e$ and $z_j e$, η_i and η_j, and r_i and r_j are the charges, number of valence shell electrons, and ionic radii of ions i and j, respectively, and ρ is the repulsion parameter ($\rho=0.29$ Å).

The charge of the Cs ion is taken equal to 1, whereas charges for boron and oxygen atoms are calculated from the following equations:

$$Z_B = 2.0 - 0.5\frac{N_{Cs}}{N_B}(1-\kappa), \tag{3}$$

$$Z_O = -1.333 - 0.5\frac{N_{Cs}}{N_O}(1-\kappa), \tag{4}$$

where $\kappa=0.667$ is a charge scaling factor that yields a partial covalent character of the B–O interactions so that the simulated vibrational spectra have a close agreement with the experimental ones.[21] N_{Cs}, N_O, and N_B are the number of Cs, O, and B atoms in a specific simulated glass composition.

An additional three-body harmonic interaction potential term for the O–B–O angles was included,

$$V_{ijk} = 0.5K_{ijk}(\theta - \theta_0)^2, \tag{5}$$

where K_{ijk} is a constant determining the strength of the interaction and θ is the angle between i–j and j–k bonds, where i and k are the oxygen atoms bonded to the jth boron atom. The angle θ_0 corresponds to the expected angle value for ideal triangular ($\theta_0=120°$) and tetrahedral ($\theta_0=109.47°$) borate units. The constant K_{ijk} assumes different values when it refers to tetrahedral ($K_{ijk}=1000$ kJ/(mol rad^2)) and triangular ($K_{ijk}=500$ kJ/(mol rad^2)) borate units. These values were determined by following the same reasoning as that for the charge scaling parameter κ. The values of parameters which appear in Eqs. (1) and (2) are summarized in Table I.

Downloaded 08 Dec 2008 to 194.177.215.121. Redistribution subject to AIP license or copyright; see http://jcp.aip.org/jcp/copyright.jsp

TABLE I. Values of ionic radii r_i and valence electrons η_i for the interatomic potential in Eqs. (1) and (2).

	r_i (Å)	η_i
B	0.770	5-z_B
O	1.265	6-z_O
Cs	1.840	8

The simulations were carried out in the canonical ensemble, where the initial configuration was generated from a random distribution of atoms over the sites of the fcc lattice with velocities taken from a Maxwellian distribution at 5000 K. Periodic boundary conditions were applied, and long-range Coulombic forces were handled by employing the Ewald summation method.[34] A fifth-order Gear predictor-corrector integrator with a time step of 0.96 fs was used.

The generated melts were quenched from an initial temperature of 5000 K to the final temperatures of 300 or 1250 K in five or three cooling cycles, respectively, where at each cycle the temperature was fixed and set equal to half of the value it had in the previous cycle. At a particular cooling cycle, temperature was monitored and kept constant for about 2 ps by scaling down the velocities of the particles at each time step, followed by another time period of 10 ps where, this time, the velocities were scaled down for every 10 time steps. In the final cooling cycle the 10-ps time period was extended to 30 ps, after which properties were accumulated for a final period of about 180 ps.

The simulated final temperatures of 300 and 1250 K correspond to the glassy state, although we have not performed calculations for the location of the exact melting point. This stems from the fact, in particular for the 1250-K temperature, that the mean-square displacement (MSD) curves of the oxygen and boron atoms are practically straight lines with a slope very close to zero. In a melt, the atoms of the network structure are expected to be more mobile. The choice of the 1250-K temperature was more or less arbitrary, and it was based on the fact that we wanted to study the temperature-induced structural changes as well as the dynamics of Cs ions not included in the present work. In a room-temperature simulated glass, the dynamics are extremely slow to be followed in a reasonable computational time.

III. RESULTS AND DISCUSSION

A. Composition and temperature dependence of the short-range order structure

The boron–oxygen radial distribution functions (RDFs) of the simulated xCs_2O-$(1-x)B_2O_3$ glasses were calculated at temperatures of 300 and 1250 K in order to determine the short-range order structure of the borate network. Typical results concerning the first peak in the boron–oxygen RDF $g_{B-O}(R)$ are shown in Fig. 1 and are compared with corresponding RDFs obtained previously for Li borate glasses.[29] This first peak in the $g_{B-O}(R)$ arises from the nearest-neighbor B–O correlations and should be taken as resulting from the overlapping contributions of B–O distances in SRO units, i.e., borate triangles ($B\emptyset_3$, $B\emptyset_2O^-$, and $B\emptyset O_2^{2-}$) and tetrahedra ($B\emptyset_4^-$). The presence of borate triangles and tetrahedra as the network building blocks is consistent with the O–B–O angle distribution functions which exhibit sharp peaks at ca. 120° and 110° for all compositions and temperatures investigated.

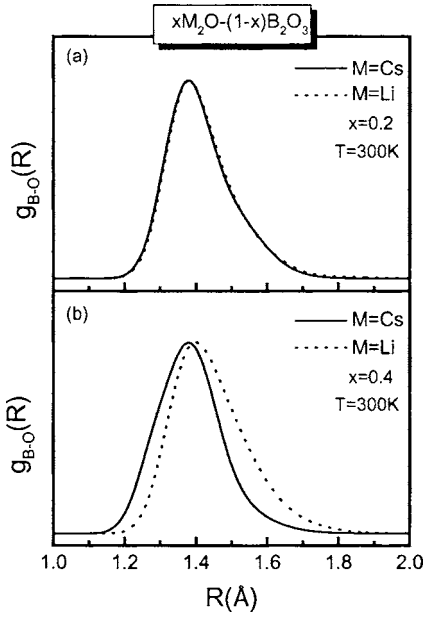

FIG. 1. The first peak of the boron–oxygen radial distribution functions at 300 K for simulated xM_2O-$(1-x)B_2O_3$ glasses (M=Cs, Li, and x=0.2, 0.4).

For the composition $x=0.2$ the first peak of $g_{B-O}(R)$ is practically independent of the nature of the alkali ion [Fig. 1(a)], implying very similar SRO structures for the two glasses. However, at higher alkali contents the fist peak exhibits a metal ion dependence as observed in Fig. 1(b) for $x=0.4$. For M=Cs the first peak appears shifted to lower B–O distances compared to those for M=Li. This peak originates from three different contributions corresponding to B(3)–NBO bonds, B(3)–Ø bonds, and B(4)–Ø bonds, where the number in parentheses denotes the coordination of the boron atom. Since the B(3)–NBO bonds are shorter than the B(3)–Ø bonds, which in turn are shorter than the B(4)–Ø bonds,[21,22] we infer that the $x=0.4$ Cs borate glass exhibits a smaller relative population of $B\emptyset_4^-$ units and a larger abundance of NBO-containing units than does its Li counterpart.

To quantify the above observations we proceed with the evaluation of the molar fraction of the SRO structural units constituting the borate network. From the integration of the first peak of $g_{B-O}(R)$ (Fig. 1) up to the first minimum, the average coordination number of boron $\langle B(O)\rangle$ is obtained, and this leads to the fraction of the $B\emptyset_4^-$ tetrahedra by the simple relation $X_4=\langle B(O)\rangle-3$. The results are displayed in Fig. 2 where they are compared with the theoretical curve $x/(1-x)$, the room-temperature NMR data for Cs borate glasses,[16,25] and the X_4 data from the MD simulation of Li borate glasses.[28,29] At $T=300$ K both experimental and MD-derived X_4 values deviate from the theoretical curve, and this effect becomes more pronounced for the $x=0.3$ and 0.4 Cs borate compositions, implying an increasing fraction of NBO-containing units at these higher Cs modification levels.

The presence of NBOs at $T=300$ K for $x=0.3$ and 0.4

Downloaded 08 Dec 2008 to 194.177.215.121. Redistribution subject to AIP license or copyright; see http://jcp.aip.org/jcp/copyright.jsp

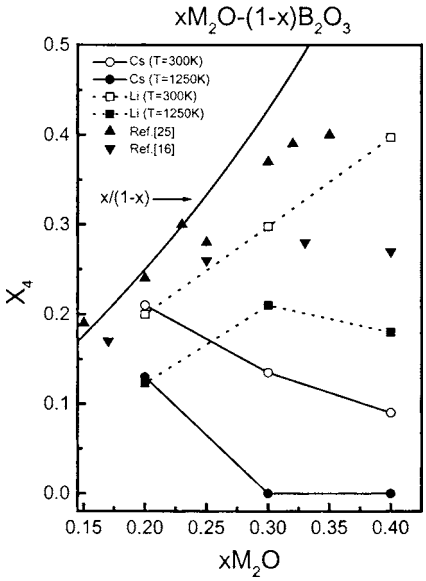

FIG. 2. Molar fraction of $B\emptyset_4^-$ tetrahedral units, X_4, in simulated Cs and Li borate glasses as a function of composition and temperature. Experimental room-temperature NMR data reported for Cs borate glasses are also included (Refs. 16 and 24). The $x/(1-x)$ curve gives the X_4 fraction if $B\emptyset_4^-$ tetrahedra are the only charged units existing in borate glasses.

could be responsible also for the larger differences in X_4 observed between experimental and MD data. As discussed by Soules[35] and others,[21,22] the very high cooling rates involved in MD simulations lead to simulated glasses having higher fictive temperatures with typical laboratory glasses. The result of this effect is that a simulated glass reflects the quasiequilibrium structure arrested at high temperatures. As shown by statistical-mechanical calculations[36] and by spectroscopic techniques, such as NMR,[37] infrared,[38] x-ray diffraction,[39] and Raman,[40] the NBO-containing triangular units of modified borate glasses are favored at high temperatures at the expense of the $B\emptyset_4^-$ tetrahedra. A similar effect of temperature was found in a recent MD simulation of a B_2O_3 glass, in the sense that the maximum fraction of boroxol rings (ca. 33%) was observed when the simulated glass was "prepared" at low temperatures.[41] However, the nonring $B\emptyset_3$ triangles were found to be favored at higher equilibration temperatures at the expense of boroxol rings, the fraction of which drops to ca. 11%.[41] Therefore, it is reasonable to find that simulated Cs borates exhibit at 300 K lower X_4 values than do laboratory glasses investigated by room-temperature NMR, provided that the alkali content favors the formation of NBOs (i.e., compositions $x=0.3$, 0.4).

As shown in Fig. 2, the structural parameter X_4 derived by MD at 300 K for the composition with the lower Cs content ($x=0.2$) is practically the same as that obtained by room-temperature NMR.[16,25] This can be attributed to the fact that the smaller NBO concentration makes the $x=0.2$ glass structure less vulnerable to the large differences in quenching rates existing between simulated and laboratory glasses. This finding is in accord with the high-temperature Raman study of Akagi *et al.* on K borate glasses.[40] They have demonstrated that the Raman profiles of the $x=0.3$ glass/melt are much more sensitive to temperature changes than those of the $x=0.2$ glass/melt.

It is clear from the above discussion that a comparison of the X_4 data on laboratory glasses from MD simulations with those from NMR spectroscopy should be made with caution. Therefore, we suggest that it is preferable to consider trends of X_4 rather than absolute values when discussing the structure of simulated glasses. In this context, the MD data in Fig. 2 indicate that for $x=0.2$ similar SRO structures exist in Li and Cs borate glasses, in agreement with the NMR findings of Berryman *et al.*[25] However, the results of the simulations for glasses of higher metal oxide contents ($x=0.3$, 0.4) indicate larger fractions of NBO-containing units in Cs glasses, in agreement with the NMR work of Zhong and Bray[16] and Bray,[17] the suggestions of Kodama and Kojima,[26] and the trend found in the neutron-scattering study of Majerus *et al.* for diborate glasses ($x=0.33$).[24]

The effect of temperature on structure is studied here by "preparing" simulated Cs borate glasses at 1250 K. In comparison with the MD data at 300 K (Fig. 2) it is clear that X_4 decreases with increasing temperature for all Cs borate compositions, in agreement with our earlier simulations of Li borate glasses[28,29] and neutron-scattering experiments on alkali diborate glasses.[24] The effect of temperature is particularly drastic for Cs contents $x=0.3$ and 0.4, since for these compositions the $B\emptyset_4^-$ tetrahedra have been completely transformed into NBO-containing borate triangular units at 1250 K. The nature of these latter units will be discussed in the following section.

Such a change in boron speciation with temperature is expected to contribute largely to the configurational entropy of the system, and, thus, it should manifest itself in structure-related properties including ion transport and viscous flow.[37] Indeed, even in early studies[9] the transformation of the $B\emptyset_4^-$ tetrahedra into triangles with NBO atoms was correlated with the reduction of network crosslinking and the consequent reduction of viscosity. More recently, Angell introduced the concept of "strength and fragility" to classify glass-forming liquids in terms of their temperature dependence on viscosity η.[42] A convenient measure of the ease with which the structure changes with temperature ("fragility" index) is the slope of the log η versus the T_g/T curve in the vicinity of glass transition (i.e., $S=\lim_{T_g/T\to 1} d\log\eta/d(T_g/T)$), as this quantity is proportional to an activation energy for viscous flow. The fragility index has been determined for Li borate glasses and was found to increase with increasing alkali oxide content.[43] In a similar approach, the activation entropy at the glass transition was used as a measure of the fragility of the system and was found also to increase with increasing alkali content in borate glasses.[44] These trends can be attributed at large to an increasing effect of temperature on the change of boron coordination from four to three with increasing alkali content as found in the MD simulations of Cs and Li borates.

B. Nonbridging oxygen (NBO)-containing borate units and NBO–NBO correlations

Considering the important role of NBOs in metal ion network bonding and transport properties,[29,45,46] it is of interest to examine the nature of NBO-containing structural

Downloaded 08 Dec 2008 to 194.177.215.121. Redistribution subject to AIP license or copyright; see http://jcp.aip.org/jcp/copyright.jsp

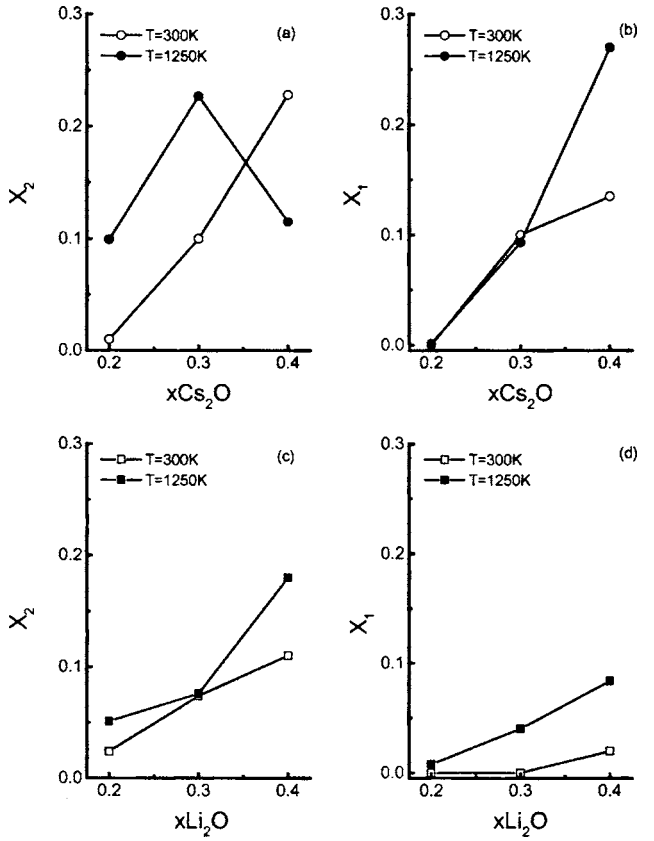

FIG. 3. Molar fractions of $B\emptyset_2O^-(X_2)$ and $B\emptyset O_2^{2-}(X_1)$ units in simulated Cs and Li borate glasses as a function of alkali content and temperature.

units in simulated Cs borate glasses. For the compositions investigated in this work the charged triangular borate units are those with one NBO ($B\emptyset_2O^-$) and two NBOs per boron ($B\emptyset O_2^{2-}$) and molar fractions X_2 and X_1, respectively. An oxygen atom is identified as NBO if no other boron atom is found within a sphere of ca. 2 Å radius. This cutoff distance corresponds to the first minimum of the B–O RDF curve, and it is found to be almost temperature and composition independent. Having determined the total number of NBO atoms in the simulated box, the fractions X_2 and X_1 were derived using the procedure described previously in detail.[29] The obtained fractions X_2 and X_1 are presented in Figs. 3(a) and 3(b) as functions of composition and temperature and are compared with the data for Li borate glasses in Figs. 3(c) and 3(d). It is evident that for $x=0.2$ the increase in temperature results in the transformation of $B\emptyset_4^-$ units into triangular $B\emptyset_2O^-$ units (fraction X_2) for both glass systems. This temperature effect on SRO speciation can be described by the isomerization reaction,

$$B\emptyset_4^- \Leftrightarrow B\emptyset_2O^-, \tag{6}$$

which shifts to the right with increasing temperature.[36–40]

The conversion of $B\emptyset_4^-$ tetrahedra into $B\emptyset_2O^-$ and $B\emptyset O_2^{2-}$ units is favored in both systems upon increasing temperature when $x>0.2$, with Cs borate glasses exhibiting larger X_2 and X_1 values than do their Li borate counterparts (Fig. 3). While the formation of $B\emptyset_2O^-$ is understood in terms of equilibrium (6), the creation of the doubly charged $B\emptyset O_2^{2-}$ units at high temperatures can result from the disproportionation reaction,

$$2B\emptyset_4^- \Leftrightarrow B\emptyset O_2^{2-} + B\emptyset_3, \tag{7}$$

which was found to operate in magnesium borate glasses.[47]

Room-temperature Raman studies[48,49] of Cs borate glasses have shown that in the range $0.3 \leqslant x \leqslant 0.5$ the negative charge is located mainly on the metaborate species, i.e., on tetrahedra $B\emptyset_4^-$ and $B\emptyset_2O^-$ triangles, the latter being organized mostly into metaborate rings $B_3O_6^{3-}$, through the following equilibrium reaction:

$$3B\emptyset_2O^- \Leftrightarrow B_3O_6^{3-}. \tag{8}$$

For Cs_2O contents approaching the metaborate composition ($x=0.5$) the room-temperature Raman spectra suggested also the presence of a small concentration of pyroborate dimers $B_2O_5^{4-}$ resulting from the $B\emptyset O_2^{2-}$ species

$$2B\emptyset O_2^{2-} \Leftrightarrow B_2O_5^{4-}. \tag{9}$$

Since Figs. 3(a) and 3(b) suggest that species $B\emptyset_2O^-$ and $B\emptyset O_2^{2-}$ exist in considerable concentrations at high Cs_2O contents and temperatures, we search now for the possibility of these SRO units being organized into well-defined medium-range-order (MRO) structures like ring and dimer types expressed by reactions (8) and (9), respectively. For this purpose, we have counted all possible structural configurations of two interconnected borate triangular units, with at least one of them being charged. These structures are termed as (*i-j*), where *i* and *j* indicate the number of NBOs per borate triangle. For example, in the structure (1-2) the first triangle has one NBO and the second one two. For the $x=0.2$ composition practically all $B\emptyset_2O^-$ units were found in configuration 1-0. For Cs_2O contents larger than $x=0.2$ the configuration 1-0 is still present, and types 1-1, 2-0, and 1-2 are also formed in percentages depending on temperature and composition. However, no tendency was found for the formation of metaborate rings or pyroborate dimers (structure 2-2) at any composition and temperature studied here. This reinforces the fact expressed above that simulated Cs borate glasses have much higher fictive temperatures than laboratory glasses, and, thus, equilibria (8) and (9) are shifted to the left in simulated glasses. This result is analogous to that reported for glassy B_2O_3 where the boroxol rings (MRO structures) were found to be dismantled into $B\emptyset_3$ triangles (SRO species) when the glass is prepared at high temperatures.[41]

Further insights into the relative organization of the NBO-containing triangles in glass can be obtained from the consideration of the NBO–NBO correlation functions, an example of which is displayed in Fig. 4 for the $x=0.3$ Cs and Li borate compositions at $T=1250$ K. The first narrow peak at ca. 2.25 Å can be attributed to correlations between NBO atoms belonging to the same triangular unit,[29] and its area is connected directly to the number of $B\emptyset O_2^{2-}$ units. A comparison of the two glasses shows that the Cs borate peak is shifted to a smaller distance, suggesting differences in bonding in the two glass systems. In particular, since the O–B–O angles of the triangular borate units remain the same in the

Downloaded 08 Dec 2008 to 194.177.215.121. Redistribution subject to AIP license or copyright; see http://jcp.aip.org/jcp/copyright.jsp

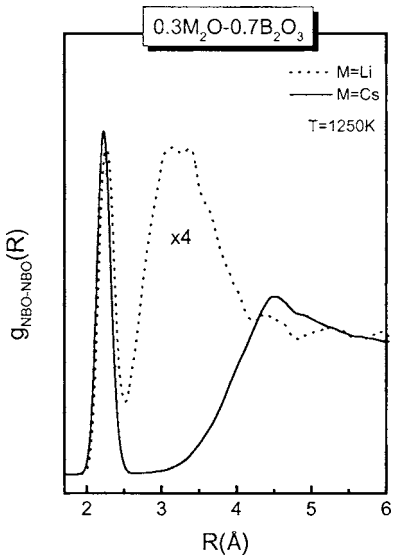

FIG. 4. NBO–NBO correlation functions for Li and Cs borate glasses of composition $0.3M_2O$–$0.7B_2O_3$ and temperature $T=1250$ K. The curves are normalized to the average total number of NBO atoms. The RDF curve for $M=$Li is multiplied by four for clarity.

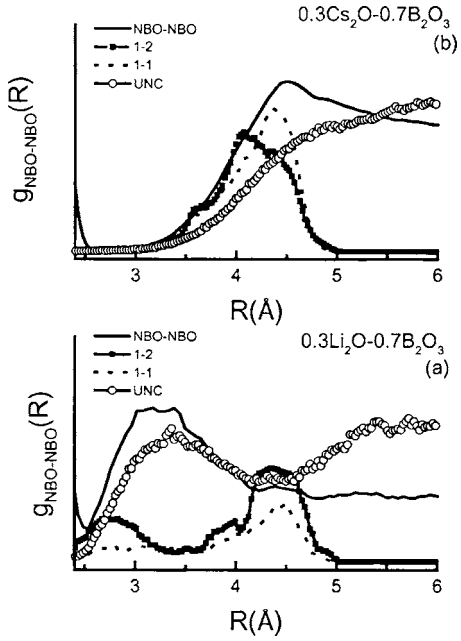

FIG. 5. NBO–NBO correlation functions for the $0.3M_2O$-$0.7B_2O_3$ glass at $T=1250$ K with $M=$Li (a) and $M=$Cs (b). Partial NBO–NBO RDF curves for configurations 1-1 and 1-2 shown in Fig. 4 also included, while the partial denoted by unc corresponds to unconnected triangular $B\emptyset_2O^-$ units. The partial RDF curves are magnified for clarity.

two systems, the smaller NBO–NBO distance found for Cs borates should be attributed to a corresponding smaller B–NBO distance. This result is consistent with the smaller field strength of Cs ion compared to Li, that leads to weaker Cs ion–oxygen interactions and, thus, to a relatively stronger B–NBO bonding in Cs glasses. As a result, the overall boron–oxygen bonding in glasses containing NBOs is expected to be stronger in Cs than in Li borates, and this is demonstrated clearly by the first peak of the B–O RDF in Fig. 1(b).

More pronounced differences in the NBO–NBO RDFs of two glass systems are observed at larger R values, where the strong peak at ca. 3.3 Å observed for the Li borate glass appears to be missing for $M=$Cs. In our previous work[29] the 3.3-Å peak was attributed to correlations between NBOs in connected borate triangles, like the structural arrangement $^-O\emptyset B\emptyset B\emptyset O^-$ found in Cs borates (configuration 1-1). However, the absence of such a peak in the Cs borate NBO–NBO correlations necessitates the reevaluation of our previous assignment. For this purpose we have calculated separately the NBO–NBO RDFs for NBO atoms belonging to connected triangular units (configurations 1-1 and 1-2), as well as to unconnected $B\emptyset_2O^-$ triangular units. The results for the $x=0.3$ Li glass at $T=1250$ K are shown in Fig. 5(a), where it is clearly shown that the major contribution to 3.3 Å comes from NBO–NBO correlations in unconnected $B\emptyset_2O^-$ units (noted by unc in Fig. 5), with such NBOs participating most likely in the coordination sphere of the same Li ion. Therefore, the high intensity of the 3.3-Å peak is another manifestation of the NBO clustering observed in Li borate glasses.[29] Interesting enough, the NBO atoms in connected borate triangles contribute mainly at ca. 4.4 Å and give rise to the small peak observed at this range in the total NBO–NBO RDF.

For the Cs-containing glass the NBO–NBO pair correlations in configurations 1-1 and 1-2 are found to peak also between 4 and 4.5 Å [Fig. 5(b)]. However, the NBO–NBO correlation function between unconnected triangular units in the Cs glass gives an increasing contribution for distances above ca. 3.5 Å, instead of the peak observed for $M=$Li. This shows that the most probable distances between NBO atoms belonging to unconnected $B\emptyset_2O^-$ configurations become now significantly larger because of the larger ionic radius of Cs, and, thus, the shell corresponding to second neighbors is not well defined.

C. Cs ion hosting sites and their short-time dynamics

The structural differences discussed above between Cs and Li borates are expected to be reflected on the metal ion–oxygen bonding characteristics. Such differences are revealed by the total alkali metal–oxygen pair radial distribution functions $g_{M-O}(R)$, which are found to peak at 3.25 Å for $M=$Cs and at 2.12 Å for $M=$Li for the room-temperature simulated glasses.

Further distinction can be made on the basis of the nature of oxygen atoms forming the coordination environment/site of the metal ion. In the previous work[29] we have shown that metal ion hosting sites can be classified according to whether they consist exclusively of bridging oxygen atoms (b-type sites) or of both bridging and nonbridging oxygen atoms (nb-type sites). Based on this classification we label individual Cs ions as Cs^b or Cs^{nb} if they reside predominantly (i.e., more than 75% of the simulation time) in b- or nb-type sites, respectively. The Cs ions which do not fulfill this criterion are considered mixed Cs^m. The fractions of Cs^b, Cs^{nb}, and Cs^m ions have been evaluated, and the results are presented in Fig. 6 as functions of composition and temperature. The population of the Cs^{nb} ions is found to increase with Cs_2O content and temperature at the expense of the Cs^b

Downloaded 08 Dec 2008 to 194.177.215.121. Redistribution subject to AIP license or copyright; see http://jcp.aip.org/jcp/copyright.jsp

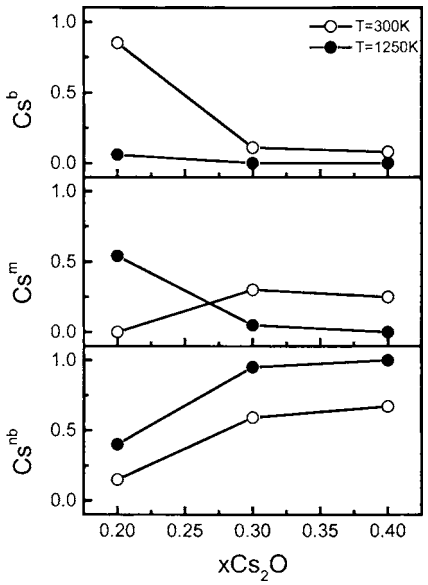

FIG. 6. Composition and temperature dependence of the mole fractions of Cs ions occupying different types of network sites: *b* type (Cs^b) nb type (Cs^{nb}), and mixed type (Cs^m). For details on the nature of the Cs ion hosting sites see text.

fraction. This result is in agreement with the progressive transformation of the $B\emptyset_4^-$ tetrahedra into NBO-containing triangles upon increasing Cs_2O content and temperature, as discussed above.

From Fig. 6 we infer that the $B\emptyset_4^-$ units are less effective than the NBO-containing units in retaining Cs ions in their vicinity for the entire simulation time. To support this argument we examine the $x=0.3$ and 0.4 compositions at $T=300$ K where a sufficient NBO concentration is present. If we suppose that each $B\emptyset_4^-$ unit is associated with one Cs ion, then the Cs^b fractions should be 0.30 and 0.15 for $x=0.3$ and $x=0.4$, respectively, according to the percentage of the $B\emptyset_4^-$ tetrahedra with respect to the total negative charge, $x/(1-x)$. However, we find that the corresponding fractions for Cs^b are 0.11 and 0.08 (Fig. 6). Similarly, the Cs^{nb} fractions would be 0.70 and 0.85 if each NBO atom were associated with one Cs cation. Instead, we find from Fig. 6 that the Cs^{nb} fractions are 0.60 and 0.67. Thus, there is a roughly 50% deviation of the calculated Cs^b fractions from the expected ones, while the corresponding deviation of the Cs^{nb} fraction is about 20%. These deviations are compensated by the presence of a significant number of Cs ions in mixed sites (Cs^m ions in Fig. 6). These findings suggest that Cs ions are loosely bonded to $B\emptyset_4^-$ tetrahedral units, and they are dragged to mixed-type environments consisting of both $B\emptyset_4^-$ and NBO-containing units.

The situation is different for the $x=0.2$ Cs borate composition at $T=300$ K, where the $B\emptyset_4^-$ tetrahedral units constitute the vast majority of the charged species (85%). We find in this case that there is a one-to-one correspondence between $B\emptyset_4^-$ tetrahedral and Cs^b ions, as well as between NBO atoms and Cs^{nb} ions. This is attributed to the reduced probability of a $B\emptyset_4^-$ tetrahedron to be in the neighborhood of a NBO atom when the alkali content and temperature are considerably low. On the other hand, NBO-containing units are able to retain Cs ions in their neighborhood despite the fact that they are minority borate species, probably a result of their higher charge density with respect to *b*-type sites.

A similar analysis for Li borate glasses[29] shows that at $T=300$ K the population of Li^b ions is considerably smaller than the population of $B\emptyset_4^-$ units, whereas the population of Li^{nb} ions is systematically larger than the number of NBO atoms. This effect was associated with a tendency of the nonbridging oxygen atom to coordinate more than one Li ion. However, as we have seen above such a trend for NBO/metal ion clustering does not seem to be pronounced in Cs borate glasses.

The classification of Cs ions according to the site where they predominantly reside and the use of the relevant pair radial distribution functions permit the evaluation of the corresponding coordination numbers with oxygen, $Cs^{nb}(O)$ and $Cs^b(O)$. It is noted that for Li borate glasses the Li^{nb}–O and Li^b–O partial RDFs show considerable differences regarding their shape and the position of the first peak (1.92 and 2.12 Å, respectively).[29] In the present case, however, the Cs^{nb}–O and Cs^b–O partial RDFs show their first peak at approximately the same position as the total Cs–O RDF (ca. 3.25 Å), the only difference being that the Cs^{nb}–O RDF is better defined than the Cs^b–O partial. Consequently, for $x=0.3$ and 0.4 and $T=300$ K the calculated coordination numbers are $Cs^{nb}(O)=9.2$ and $Cs^b(O)=11.6$ for cutoff distances of 4.1 and 4.4 Å, respectively, from the particular Cs ion. For other compositions and temperatures the Cs^{nb} or Cs^b population is not adequate to obtain statistically reliable results. The coordination numbers for Cs ions found in this work are considerably larger than those for Li ions, $Li^{nb}(O)=5.5$ and $Li^b(O)=8$,[29] and this is fully consistent with the size difference of Cs and Li ions. The average Cs(O) coordination number is about ten in very good agreement with results reported for crystalline Cs triborate.[50]

In the following, we examine whether the distinction of Cs ions into Cs^b and Cs^{nb} types is reflected also in their vibrational properties. The vibrational density of states $\Phi(\omega)$ of metal ions in glass can be calculated from the Fourier transform of their velocity autocorrelation function $\Phi(t)$ obtained from the following expression:

$$\Phi(t)=\left\langle \frac{1}{N}\sum_{j=1}^{N}\vec{v}_j(t)\vec{v}_j(0)\right\rangle, \tag{10}$$

where $\vec{v}_j(t)$ is the velocity of metal ion j at time t and N is the number of metal ions.[21,29,46] We have applied this formalism to calculate separately the $\Phi(\omega)$ for Cs^b and Cs^{nb} ions. The results for $x=0.4$ and $T=300$ K are reported in Fig. 7(a) and are compared with the experimental far-infrared spectrum of the $x=0.33$ Cs borate glass.[20] As shown, the $\Phi(\omega)$ responses for Cs^b and Cs^{nb} ions are in the far-infrared region are quite broad. Nevertheless, they are clearly distinguished and the spectral weight attributed to Cs^{nb} ions contributes mostly to the high-frequency part of the spectrum, whereas the response of Cs^b ions is active mainly at lower frequencies. This result strongly supports previous findings for the vibrational properties of lithium ions in borate glasses,[29] in the sense that the distinction of metal ions according to the nature of

Downloaded 08 Dec 2008 to 194.177.215.121. Redistribution subject to AIP license or copyright; see http://jcp.aip.org/jcp/copyright.jsp

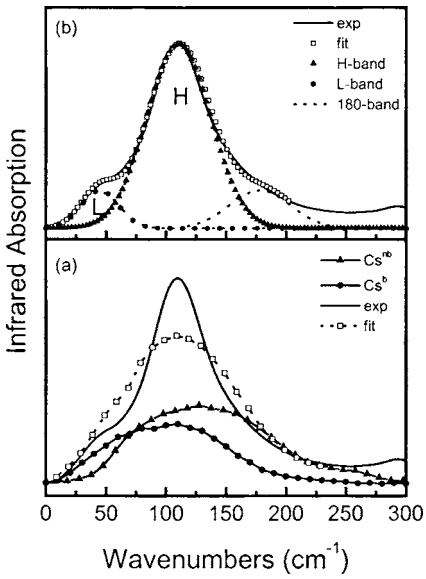

FIG. 7. (a) Calculated power spectra of Cs ions in bridging-type (Cs^b) and nonbridging-type (Cs^{nb}) sites in the simulated $0.4Cs_2O$-$0.6B_2O_3$ glass at $T=300$ K. A linear combination of the power spectra is shown for comparison with the experimental far-infrared spectrum of the $0.33Cs_2O$-$0.67B_2O_3$ glass. (b) The experimental far-infrared absorption profile shown in (a) is deconvoluted into Gaussian components (denoted by *L* and *H*) originating from Cs–O vibrations in different local environments. The third component band at ca. 180 cm^{-1} was attributed (Ref. 20) to libration modes of disconnected segments of the borate network.

their sites in glass is very well reflected also in their short-time dynamics. In addition, these findings are in line with our earlier analysis of experimental far-infrared spectra into two component bands [*L* and *H* in Fig. 7(b)], and their assignment to the alkali ion site vibrations in at least two distributions of ion hosting sites.[20,51] This work allows now a more detailed description of bands *H* and *L* in terms of the Cs–O vibrations in nb- and *b*-type sites, respectively.

IV. CONCLUSIONS

In a continuation of our recent work on molecular-dynamics (MD) simulations on Li borate glasses,[27–29] this paper presents MD study of xCs_2O-$(1-x)B_2O_3$ glasses as a function of composition ($0.2 \leqslant x \leqslant 0.4$) and temperature ($T=300$, 1250 K). The main purpose of the present investigation is to provide insights on the role of alkali metal ions in aspects of structure and ion dynamics. The short-range-order (SRO) units building the Cs glass network were found to be borate tetrahedra ($B\emptyset_4^-$) and triangles ($B\emptyset_3$, $B\emptyset_2O^-$, and $B\emptyset O_2^{2-}$), the latter having variable numbers of bridging ($\emptyset$) and nonbridging ($NBO=O^-$) oxygen atoms. From the analysis of the B–O and the NBO–NBO radial distribution functions the molar fractions of the SRO units were calculated and found to depend strongly on both Cs_2O content, *x*, and temperature. In particular, it was shown that the increase of *x* leads to the progressive depolymerization of the glass network by increasing the relative abundance of NBO-containing units at the expense of the $B\emptyset_4^-$ tetrahedra. This network transformation process was found to be enhanced at higher temperatures, and the extent of this effect is increased in glasses with larger alkali contents. Such structural changes were described in terms of isomerization [Eq. (6)] and disproportionation [Eq. (7)] equilibria between borate tetrahedra and triangles, and were associated with the increase of the fragile character of the glass with alkali content. Comparison of the present results with our previous study[29] shows that at $x=0.2$ the Cs and Li glasses exhibit great similarities in the type and relative population of the SRO units. However, simulated glasses with larger alkali contents ($x=0.3$, 0.4) show a dependence on alkali ion, with Cs borates having a larger tendency for NBO-containing units than do Li borate glasses. In addition, the local B–NBO and metal ion–oxygen bonding characteristics were found to vary with alkali ion. In particular, the average B–NBO bond was found to be stronger in Cs glasses and the metal ion hosting sites to involve larger coordination numbers and longer metal ion–oxygen distances than those for lithium borates. Such effects were correlated naturally with the field strength and ion size differences of the two alkali ions.

The investigation of the microstructure of Cs ion sites reveals the existence of two types of environments that retain their identity during the simulation time; the first is formed exclusively by bridging oxygen atoms (*b* type) and the second by both bridging and nonbridging oxygens (nb type). Similarly, cations are distinguished as either Cs^b or Cs^{nb} if they reside for more than 75% of the simulation time ($\sim$180 ps) in *b*-type or nb-type sites, respectively. This distinction is manifested also on the vibrational properties of Cs ions; i.e., the calculated Cs^{nb} ion site vibrational response appears at higher far-infrared frequencies than does that of Cs^b ions. This result is compatible with our previous findings for Li borates[29] and offers an explanation for the microscopic origin of the two component bands resolved previously in the experimental far-infrared spectra.

ACKNOWLEDGMENT

Partial support by the EU (Project No. HPMD-CT-2000-00033) is gratefully acknowledge.

[1] For a review article on early studies of borate glasses see: D. L. Griscom, *Borate Glasses: Structure, Properties and Applications*, edited by L. D. Pye, V. D. Frechette, and N. J. Kreidl (Plenum, New York, 1978), pp. 11–149.
[2] J. Krogh-Moe, Phys. Chem. Glasses **6**, 46 (1965).
[3] A. H. Silver and P. J. Bray, J. Chem. Phys. **29**, 984 (1958).
[4] P. J. Bray and J. G. O'Keefe, Phys. Chem. Glasses **4**, 37 (1961).
[5] G. E. Jellison, S. A Feller, and P. J. Bray, Phys. Chem. Glasses **19**, 52 (1978).
[6] W. L. Konijnendijk and J. M. Stevels, J. Non-Cryst. Solids **18**, 307 (1975).
[7] R. L. Mozzi and B. E. Warren, J. Appl. Crystallogr. **3**, 251 (1970).
[8] P. A. V. Johnson, A. C. Wright, and R. N. Sinclair, J. Non-Cryst. Solids **50**, 281 (1982).
[9] P. C. Li, A. C. Ghose, and G. J. Su, J. Am. Ceram. Soc. **45**, 83 (1962); **45**, 89 (1962).
[10] B. D. McSwain, N. F. Borelli, and G. J. Su, Phys. Chem. Glasses **4**, 1 (1963).
[11] A. J. Easteal and D. J. Udy, Phys. Chem. Glasses **14**, 107 (1973).
[12] J. A. Duffy and M. D. Ingram, J. Non-Cryst. Solids **21**, 273 (1976).
[13] K. K. Karsch, Glastech. Ber. **35**, 234 (1962).
[14] J. E. Shelby, J. Am. Ceram. Soc. **66**, 225 (1983).
[15] D. R. Uhlmann, A. G. Kolbeck, and D. L. DeWitte, J. Non-Cryst. Solids **5**, 426 (1971).
[16] J. Zhong and P. J. Bray, J. Non-Cryst. Solids **111**. 67 (1989).
[17] P. J. Bray, Proceedings of the *Second International Conference on Borate*

Downloaded 08 Dec 2008 to 194.177.215.121. Redistribution subject to AIP license or copyright; see http://jcp.aip.org/jcp/copyright.jsp

Glasses, Crystals and Melts, edited by A. C. Wright, S. A. Feller, and A. C. Hannon (Society of Glass Technology, Sheffield, UK, 1997), pp. 1–20.
[18] G. D. Chryssikos, E. I. Kamitsos, and M. A. Karakassides, Phys. Chem. Glasses **31**, 109 (1990).
[19] E. I. Kamitsos, G. D. Chryssikos, and M. A. Karakassides, Phys. Chem. Glasses **29**, 121 (1988).
[20] E. I. Kamitsos, A. P. Patsis, and G. D. Chryssikos, J. Non-Cryst. Solids **152**, 246 (1993).
[21] A. H. Verhoef and H. W. den Hartog, J. Non-Cryst. Solids **182**, 235 (1995).
[22] A. N. Cormack and B. Park, Phys. Chem. Glasses **41**. 272 (2000).
[23] R. E. Youngman and J. W. Zwanziger, J. Am. Chem. Soc. **117**, 1397 (1995).
[24] O. Majerus, L. Cormier, G. Calas, and B. Beneu, Phys. Rev. B **67**, 024210 (2003).
[25] J. R Berryman, S. A. Feller, M. Affatigato, M. Kodama, B. M. Meyer, S. W. Martin, F. Borsa, and S. Kroeker, J. Non-Cryst. Solids **293**, 483 (2001).
[26] M. Kodama and S. Kojima, *Proceedings of the Second International Conference on Borate Glasses, Crystals and Melts*, edited by A. C. Wright, S. A. Feller, and A. C. Hannon (Society of Glass Technology, Sheffield, UK, 1997), pp. 181–188.
[27] W. Clarida, J. R. Berryman, M. Affatigato, S. A. Feller, S. Kroeker, J. Ash, J. W. Zwanziger, B. Meyer, F. Borsa, and S. W. Martin, Phys. Chem. Glasses **44**, 215 (2003).
[28] C. P. E. Varsamis, A. Vegiri, and E. I. Kamitsos, Condens. Matter Phys. **4**, 119 (2001).
[29] C. P. E. Varsamis, A. Vegiri, and E. I. Kamitsos, Phys. Rev. B **65**, 104203 (2002).
[30] C. P. E. Varsamis, A. Vegiri, and E. I. Kamitsos, J. Non-Cryst. Solids **307–310**, 956 (2002).
[31] M. Royle, J. MacKenzie, J. Taylor, M. Sharma, and S. Feller, J. Non-Cryst. Solids **177**, 242 (1994).
[32] O. V. Mazurin and M. V. Streltsina, *Handbook of Glass Data* (Elsevier, New York, 1985), Pt. B.
[33] H. C. Lim and S. Feller, J. Non-Cryst. Solids **94**, 36 (1987).
[34] M. P. Allen and D. J. Tildesley, *Computer Simulations of Liquids* (Clarendon, Oxford, 1986), p.156.
[35] T. F. Soules, J. Non-Cryst. Solids **49**, 29 (1982).
[36] R. J. Araujo, J. Non-Cryst. Solids **58**, 201 (1983).
[37] J. F. Stebbins and S. E. Ellsworth, J. Am. Ceram. Soc. **79**, 2247 (1996);S. Sen, Z. Xu, and J. F. Stebbins, J. Non-Cryst. Solids **226**, 29 (1998).
[38] C. P. Varsamis, E. I. Kamitsos, and G. D. Chryssikos, Phys. Rev. B **60**, 3885 (1999).
[39] G. Herms and J. Sakowski, Phys. Chem. Glasses **41**, 309 (2000).
[40] R Akagi, N. Ohtori, and N. Umesaki, J. Non-Cryst. Solids **293–295**, 471 (2001).
[41] J. K Maranas, Y. Chen, D. K. Stillinger, and F. H. Stillinger, J. Chem. Phys. **115**, 6578 (2001).
[42] C. A Angell, J. Non-Cryst. Solids **131–133**, 13 (1991), and references therein.
[43] G. D. Chryssikos, J. A. Duffy, J. K. Hutchinson, M. D. Ingram, E. I. Kamitsos, and A. Pappin, J. Non-Cryst. Solids **172–174**, 378 (1994).
[44] S. V. Nemilov, Glass Phys. Chem. **23**, 1 (1997).
[45] G. N. Greaves and K. L. Ngai, Phys. Rev. B **52**, 6358 (1995).
[46] A. Karthikeyan and K. J. Rao, J. Phys. Chem. B **101**, 3105 (1997).
[47] Y. D. Yiannopoulos, G. D. Chryssikos, and E. I. Kamitsos, Phys. Chem. Glasses **42**, 164 (2001).
[48] E. I. Kamitsos, G. D. Chryssikos, and M. A. Karakassides, Phys. Chem. Glasses **30**, 229 (1989).
[49] E. I. Kamitsos, M. A. Karakassides, A. P. Patsis, and G. D. Chryssikos, J. Non-Cryst. Solids **116**, 115 (1990).
[50] J. Krogh-Moe, Acta Crystallogr., Sect. B: Struct. Crystallogr. Cryst. Chem. **30**, 1178 (1974).
[51] E. I Kamitsos and G. D. Chryssikos, Solid State Ionics **105**, 75 (1998).

Downloaded 08 Dec 2008 to 194.177.215.121. Redistribution subject to AIP license or copyright; see http://jcp.aip.org/jcp/copyright.jsp